

Microstructural Evolution of DP980 Steel during Friction Bit Joining

T. HUANG, Y.S. SATO, H. KOKAWA, M.P. MILES, K. KOHKONEN, B. SIEMSEN, R.J. STEEL, and S. PACKER

The authors study a new solid-state spot joining process, friction bit joining (FBJ), which relies on the use of a consumable joining bit. It has been reported that FBJ is feasible for the joining of steel/steel and aluminum/steel, but the metallurgical characteristics of the joint for enhancement of the properties and reliability remain unclear. Therefore, this study produced friction bit joints in DP980 steel and then examined the microstructures in the joint precisely. In this article, the microstructure distribution associated with hardness in the friction-bit-joined DP980 steel and the microstructural evolution during FBJ are reported.

DOI: 10.1007/s11661-009-0016-x

© The Minerals, Metals & Materials Society and ASM International 2009

I. INTRODUCTION

AUTOMOTIVE spot welding of sheet metal has become more challenging in recent years, with an increasing usage of advanced high-strength steels (AHSSs) and light metals in the fabrication of automotive structures. These efforts are driven by the requirement for the weight reduction and the performance optimization of the vehicles. The use of these materials presents challenges of formability and weldability, because AHSS has higher contents of alloying elements than lower strength steels and because light metals cannot easily be joined to AHSS by traditional resistance spot welding (RSW).

The RSW is a well-known method for joining sheet steel components in the automotive industry. However, AHSS can often experience weld property degradation when joined by RSW.^[1–5] In resistance spot welds of AHSS, and especially the steels with tensile strengths above 800 MPa, the brittle microstructure is developed in the weld nugget during RSW, which causes interfacial failure under impact loading conditions, resulting in relatively low impact resistance. In addition, the brittle microstructure phases present concerns of hydrogen-induced cracking, which could reduce the durability of a vehicle.

Friction stir spot welding (FSSW) is an alternate joining process with RSW, developed from friction stir welding (FSW), which has already been applied to welding of steels.^[6–16] This process creates the lap weld

by plunging and retracting of the welding tool, which does not accompany the travel of the tool. Compared with RSW, FSSW can reduce the thermal effect to the welded material due to the solid-state process. The FSSW has been already known as an effective and productive method for joining aluminum alloys,^[17–20] and it has been recently applied to AHSS sheet metals using the polycrystalline cubic boron nitride tool.^[21,22] Feng *et al.*^[21] have shown that FSSW can produce metallurgical bonding for both 600 MPa dual-phase steel and 1310 MPa martensitic steel under 3 seconds of welding time and that the welds exhibited similar microstructure and hardness as the base materials for both steels. However, both the lap shear and cross tension strengths are currently limited due to the relatively small bonding widths, which would be expected to be increased through further process development.

In order to resolve some difficulties of spot joining AHSS and dissimilar combinations of AHSS and aluminum, a new concept, friction bit joining (FBJ), has been developed, where a consumable joining bit is used for joining of two or more sheets.^[23] This concept relies on a cutting step, where the bit cuts through the top layer (or layers) of material, followed by a joining step where the bit and surrounding sheet materials are heated by friction and where the bit is consumed as filler material that joins the sheets together. At the end of the joining process, the spindle of the welding machine was stopped and then restarted to separate the joining bit from the weld. The schematic drawing of this process is shown in Figure 1. The shape of the tip of the joining bit is also placed in Figure 1(a). Miles *et al.*^[23] have shown the feasibility of this process for joining of steel/steel and aluminum/steel and have demonstrated the high level of lap shear strength of the joints. They showed the high potential of FBJ as a new spot welding process, *e.g.*, the higher strength in the dissimilar friction bit joint between steel and aluminum. However, the metallurgical data, which strongly affect the mechanical properties of the joint and are directly related to the reliability of the

T. HUANG, Postdoctoral Student, Y.S. SATO, Associate Professor, and H. KOKAWA, Professor, are with the Department of Materials Processing, Graduate School of Engineering, Tohoku University, Sendai 980-8579, Japan. Contact e-mail: a6td9508@stu.material.tohoku.ac.jp. M.P. MILES and K. KOHKONEN, Associate Professors, and B. SIEMSEN, Student, are with School of Technology, Brigham Young University, Provo, UT 84602. R.J. STEEL and S. PACKER, Research Scientists, are with MegaStir Technologies, Provo, UT 84604.

Manuscript submitted March 31, 2008.

Article published online October 14, 2009

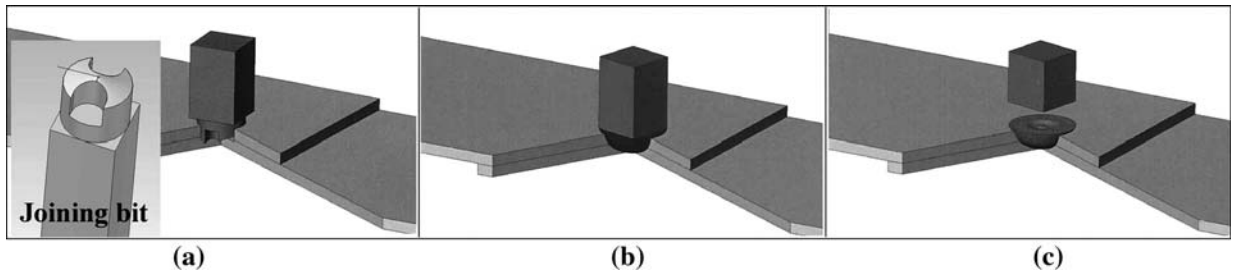


Fig. 1—Schematic illustration of FBJ process: (a) cutting step, (b) joining step, and (c) rapid stop of the spindle.

Table I. Chemical Compositions (Weight Percent) of DP980 and D2 Steel

	C	Mn	Si	Cr	S	P	Mo	V
DP980	0.15	1.44	0.32	0.02	0.007	0.011	—	—
D2	1.50	—	—	11.50	—	—	0.75	0.80

joint, have not been systematically examined yet in this joining process. In this study, therefore, the microstructure distribution associated with the hardness was examined in the similar friction bit joint of DP980 steel. Furthermore, the microstructural evolution during FBJ was also investigated.

II. EXPERIMENTAL PROCEDURES

The sheet material used in the present study was DP980 steel, 1.4 mm in thickness. The D2 tool steel, heat treated to a hardness of about 63 Rc, was used as the joining bit. Compositions of DP980 and D2 steel are provided in Table I.

The DP980 steel has a dual-phase microstructure of 48 pct martensite distributed throughout a ferrite matrix, as shown in Figure 2(a). The tensile properties of the DP980 base material are shown in Table II. The tensile specimen geometry followed the ASTM E8 sheet specification, and testing was carried out at a constant speed of 0.042 mm/s. Microstructure of D2 steel is

composed of a martensite matrix, massive carbides, and granular carbides,^[24] as shown in Figure 2(b).

The FBJ was done on DP980 sheets that were 25.4-mm wide and 101.2-mm long, with overlap of 25.4 mm in the joint area. The joints were produced in the center of the overlapped area. During the cutting procedure, the joining bit was rotated at a relatively slow speed of 725 rpm, while during the joining operation, the speed was increased to 1800 rpm. The joining bit was plunged into the sheet at 25 mm/min during the cutting step, while 100 mm/min was used during the joining operation.

Microstructure of the joint was examined by optical microscopy (OM) and scanning electron microscopy (SEM). The OM and SEM observations were carried

Table II. Tensile Properties of DP980 Base Material

Material	YS (MPa)	UTS (MPa)	Total Elongation (Pct)
DP980	703	1009	16

YS = yield strength; UTS = ultimate tensile strength.

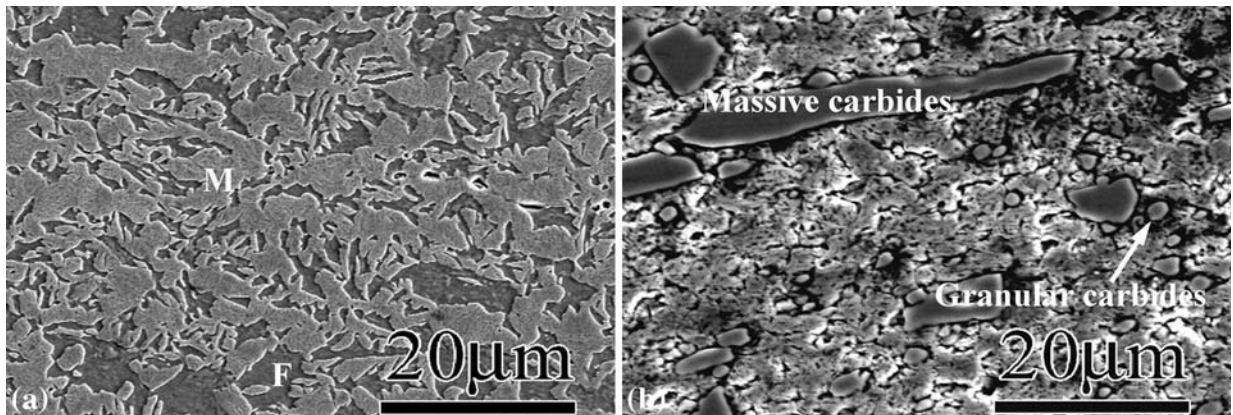


Fig. 2—SEM microstructures of base material: (a) DP980 steel and (b) D2 tool steel.

out on a cross section of the joint etched with 5 vol pct nitric acid + ethanol solution. The martensite fraction was measured by point counting for SEM image. To identify the crystallographic features of microstructure,

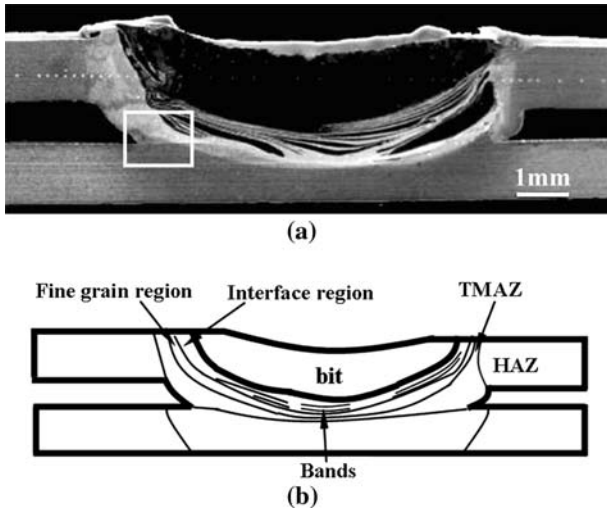


Fig. 3—(a) Macroscopic picture of cross section and (b) schematic illustration of cross section.

the electron backscattered diffraction (EBSD) method was employed. The sample for EBSD was electrolytically polished in 10 vol pct HClO_4 + 90 vol pct CH_3COOH solution at 25 V. Crystallographic data collection by EBSD was operated at 20 kV. Observation area of the equiaxed fine grain region was $50 \mu\text{m} \times 50 \mu\text{m}$ under step size of $0.25 \mu\text{m}$, while for other regions, is was $125 \mu\text{m} \times 95 \mu\text{m}$ under step size of $0.50 \mu\text{m}$. Crystallographic data were expressed as grain boundary (GB) maps. The black and gray lines correspond to the high-angle boundaries (HABs) having misorientation angles higher than 15 deg and the low-angle boundaries (LABs) having misorientation angles between 2 and 15 deg, respectively.

The Vickers hardness profile of the joint was measured at the center of the top sheet on the cross section with 500 g load for 10 seconds.

III. RESULTS AND DISCUSSION

A macroscopic overview of the cross section of the joint is presented in Figure 3. Macroscopic observation confirmed that a defect-free joint was successfully produced by FBJ. The joining bit remains in the joint, and the alternating bands are found between the bit and DP980 steel. In addition, a gap between the two sheets is

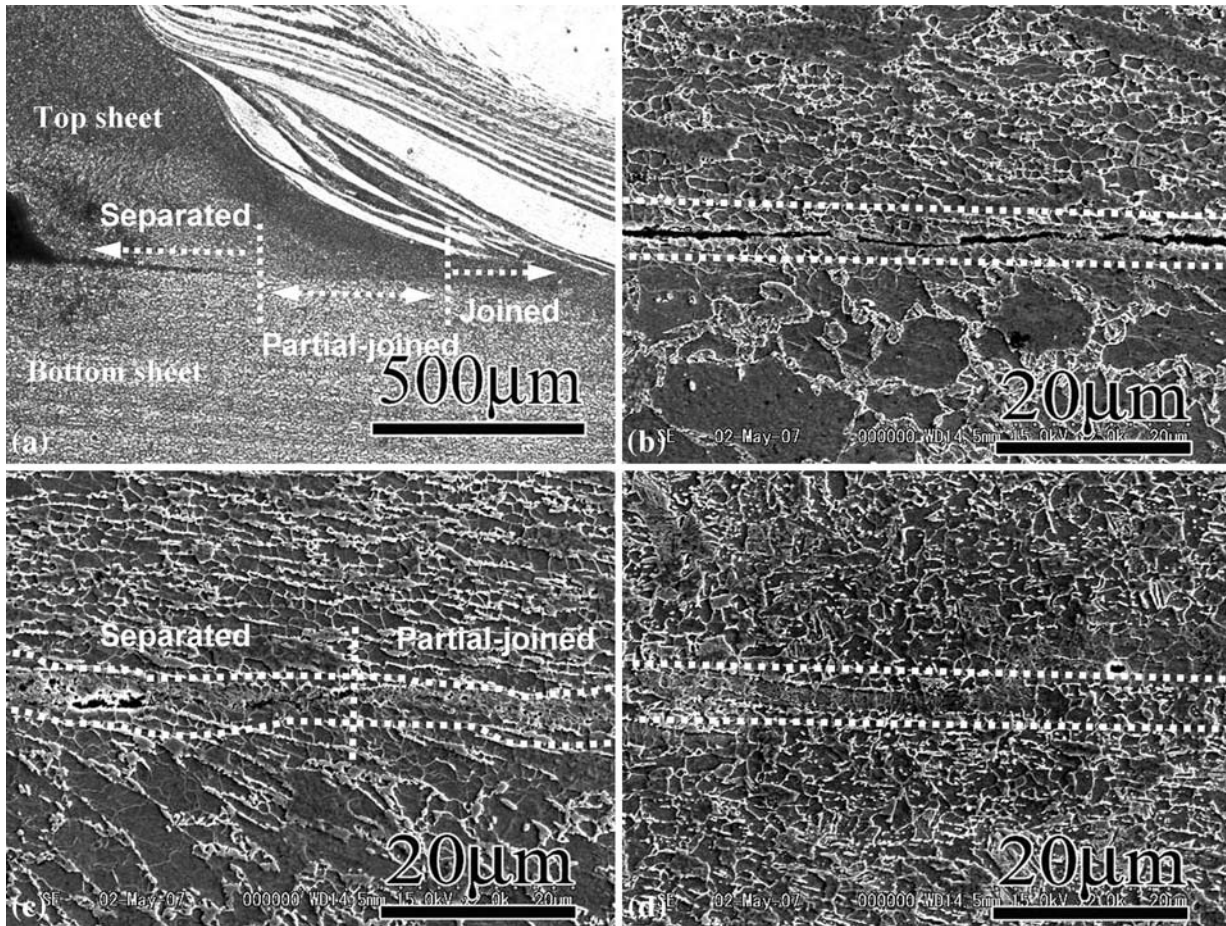


Fig. 4—(a) Interface between the top and the bottom sheets, (b) separated region, (c) partial-joined region, and (d) joined region.

found, as seen in Figure 3. This is because the clamping around the weld area was not close enough to prevent the sheets from separating during the welding. Moreover, the plunge of the bit caused some flashing of material, which might also contribute to the occurrence of a small gap.

The interface between the top and bottom sheets, which is marked by a white rectangle in Figure 3(a), is magnified in Figure 4(a). The joint interface (from left to right) is divided into three regions, according to degree of metallurgical bonding of the sheets. The separated interface, where the two sheets do not join together, is shown in Figure 4(b). In the region closer to the joint center, it seems that the metallurgical bonding

of the two sheets is partially achieved, as shown in Figure 4(c). The metallurgical bonding is mostly completed in the vicinity of the joint center, as shown in Figure 4(d).

Precise SEM examination of the microstructure revealed that the microstructures in the joint were classified into seven regions, which are shown in Figure 3(b): (1) the bit in the center of the joint, (2) the interface region just outside the bit, (3) the alternating bands located between the bit and the interface region, (4) the fine grain region closed to the interface region, (5) the thermomechanically affected zone (TMAZ) outside the fine grain region, (6) the heat-affected zone (HAZ) outside the TMAZ, and (7) the

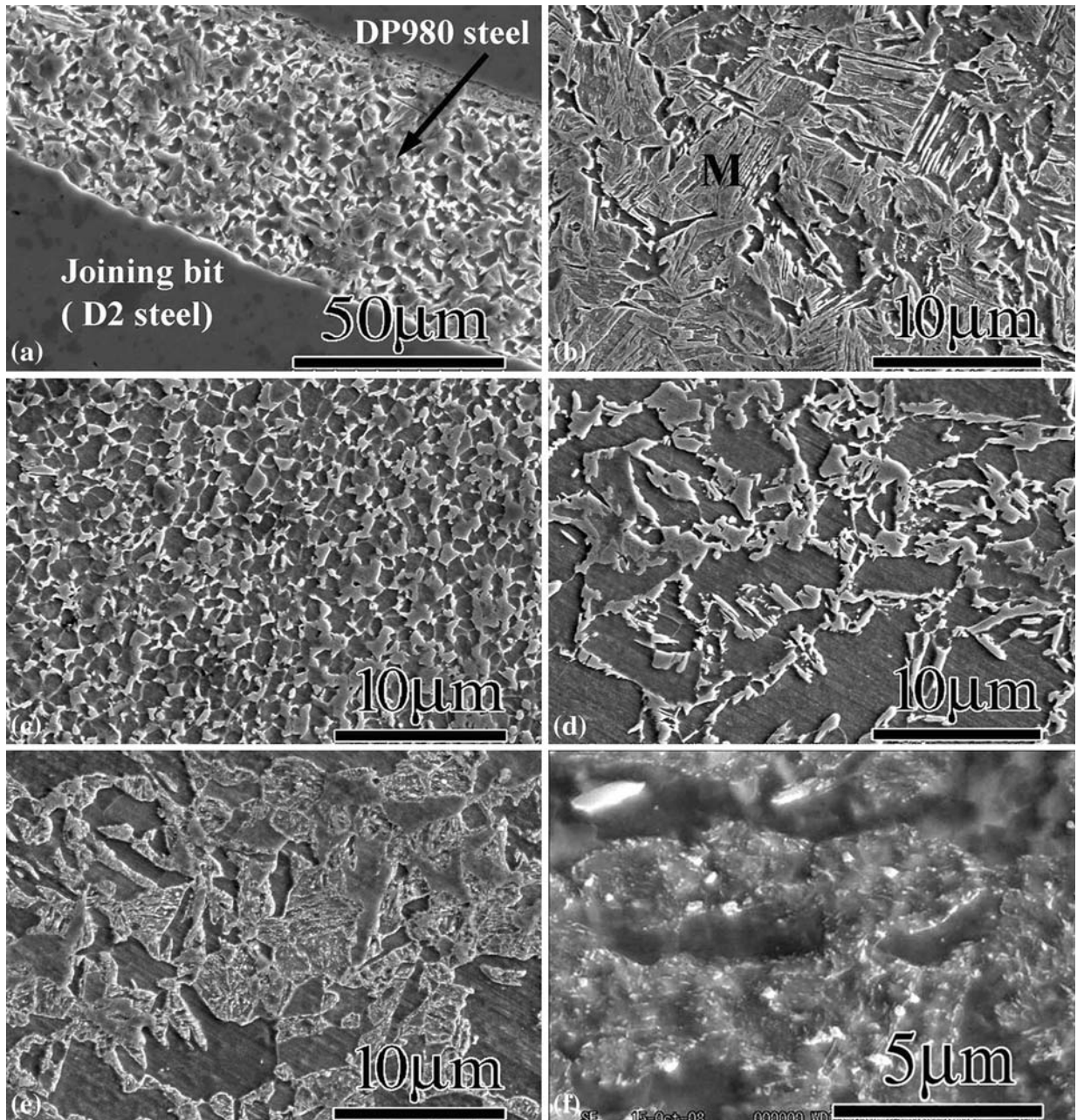


Fig. 5—Typical microstructures of (a) bands, (b) interface region, (c) fine grain region, (d) TMAZ, (e) HAZ, and (f) precipitated carbides.

unaffected DP980 base material (BM). The SEM images of the alternating bands, interface region, fine equiaxed-grain region, TMAZ, and HAZ are shown in Figure 5. The expressions “bit,” “alternating bands,” “interface region,” and “fine grain region” and the notations “TMAZ,” “HAZ,” and “BM” are used throughout this article.

The alternating bands consist of the DP980 steel and the joining bit (D2 steel) (Figure 5(a)). The martensitic structure is clearly observed in the DP980 steel region of the bands. The interface region also mainly has the martensitic structure (Figure 5(b)). Figure 5(c) shows the fine grain region consisting of fine ferrite and martensite. Both the ferrite grains and martensite clusters look equiaxed, and the martensite fraction was about 55 pct in this region. The lath martensite with the ferrite matrix is found in the TMAZ, and its martensite fraction is about 50 pct, as shown in Figure 5(d). The HAZ has roughly the same microstructure as the BM, but the carbide precipitation is observed in the martensite (Figure 5(e)). The higher magnification view of the precipitated carbides is shown in Figure 5(f).

A typical Vickers hardness profile of the joint is given in Figure 6. The DP980 base material has average hardness of about 280 HV, while the average hardness of the joining bit (D2 steel) is quite high (about 700 HV) due to the martensitic structure of steel with the higher carbon content. Outside the bit, the hardness in the side of the DP980 steel is maximal in the interface region. The hardness decreases from the interface region toward the HAZ and then increases toward the BM. The lowest hardness is found in the HAZ near the TMAZ.

Microstructural evolution of each region during FBJ could be explained as follows. Previous studies on FSW of steel^[8,25,26] have shown that the maximum temperature generally exceeded the A_3 temperature in the steels during FSW. Moreover, it is well known that the maximum temperature during friction welding is close to the melting temperature of the material to be welded.^[27–29] The DP980 steel was friction welded with the joining bit during FBJ, so that the

maximum temperature should be much higher than the A_3 temperature at the joining step.

Since the interface region is located beside the joining bit, it would experience both frictional heating and severe plastic deformation during the joining step of FBJ. Additionally, the maximum temperature should be higher than the A_3 temperature in this region. Thus, the austenite single-phase structure is formed during the joining step and then transforms into the martensitic structure during the cooling cycle. This microstructural change during FBJ would cause the high hardness of the interface region.

The fine grain region had a mixed microstructure consisting of fine ferrite grains and martensite clusters. Since the martensite clusters are formed by cooling of the austenite ones, this region would have the fine (ferrite + austenite) structure at the joining step. Fujii *et al.*^[8] showed that very fine (ferrite + pearlite) structure is formed in friction-stir-welded carbon steels when FSW is performed at the (ferrite + austenite) temperature range, which suggests that the fine (ferrite + martensite) structure can be created through intense deformation at the (ferrite + austenite) stable temperature range. From this situation, it is suggested that the fine grain region in the joint was intensively deformed at the (ferrite + austenite) stable temperature region during the joining step of FBJ. A GB map of the fine grain region is given in Figure 7. This study could not distinguish ferrite and martensite through EBSD analysis, because their crystallographic structures are very close, but this figure clearly shows the fine grain structure with a low density of LABs in the fine grain region. This map implies that the fine equiaxed grains are produced in this region through dynamic recrystallization of the (ferrite + austenite) structure during FBJ.

The TMAZ had a mixed microstructure consisting of ferrite and martensite (Figure 5(d)). This microstructure would be formed also by the cooling of the (ferrite + austenite) structure during FBJ; *i.e.*, the

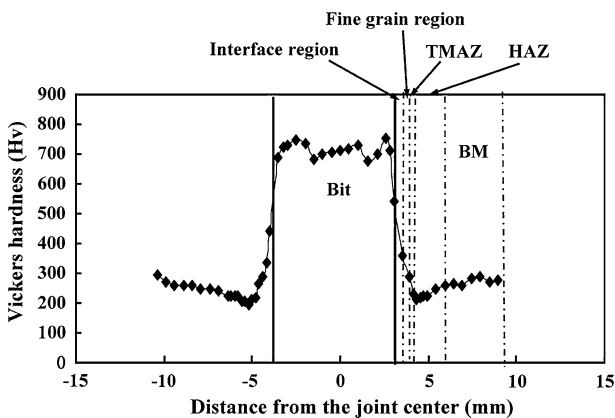


Fig. 6—Microhardness profile of cross section in the center of the top sheet.

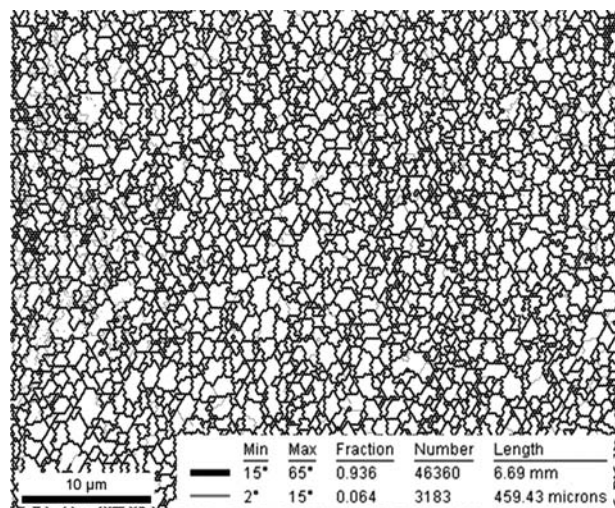


Fig. 7—Grain boundary map of the fine grain region.

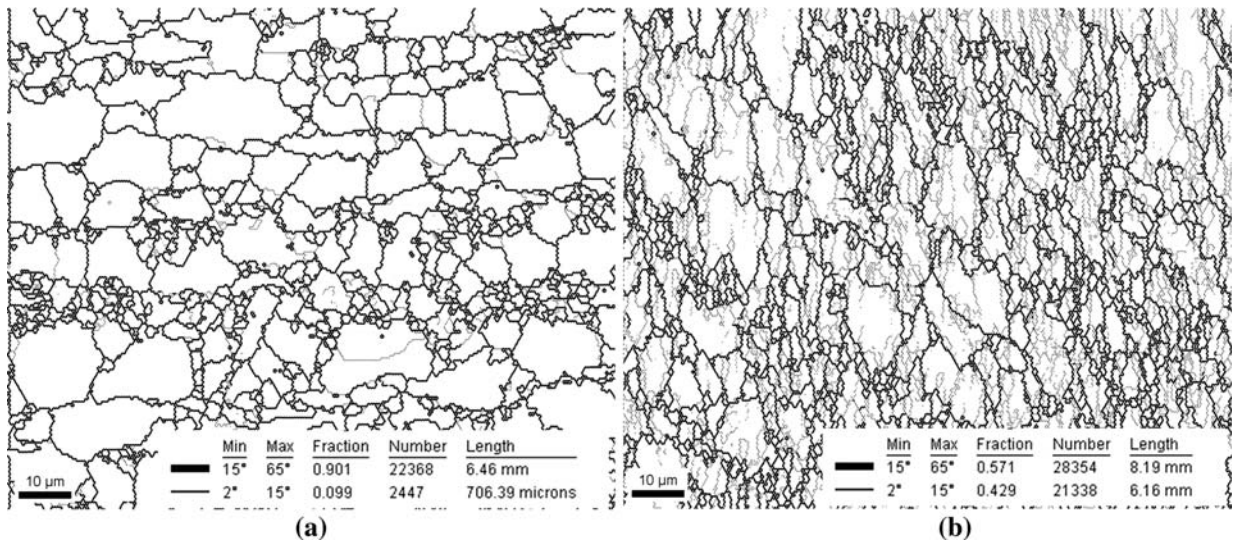


Fig. 8—Grain boundary maps of (a) BM and (b) TMAZ.

TMAZ is also heated to the (ferrite + austenite) stable temperature range as well as the fine grain region, but the maximum temperature should be lower in the TMAZ due to its greater distance from the joining bit. Since the austenite fraction decreases with temperature in the (ferrite + austenite) stable temperature range, a decrease in martensite fraction from the fine grain region toward the TMAZ can be reasonably explained. The GB maps of the BM and TMAZ are shown in Figure 8. Comparison between the SEM image and the GB map suggests that large grains in the map are ferrite. The ferrite in the BM hardly contains the LABs, while the TMAZ has the elongated ferrite with a high density of LABs. This result means that the TMAZ was also somewhat deformed during FBJ, but the introduced strain and temperature are insufficient for recrystallization, which results in remnants of the thermomechanical effect in the ferrite grain interiors of the TMAZ.

Hardness decreased from the interface region toward the TMAZ in the DP980 steel, as shown in Figure 6. The SEM images (Figure 5) clearly showed the decrease in martensite fraction from the interface region toward the TMAZ, which is directly related with the maximum temperature during FBJ. In the carbon steels, it has been reported that the hardness mainly depends on the martensite fraction.^[6,30] Therefore, reduction of the hardness from the interface region toward the TMAZ in the joint can be explained also by the martensite fraction.

The HAZ had roughly the same grain structure as the BM, but carbide precipitation was observed in the martensite region. This result suggests that the martensite in the duplex microstructure of the BM was tempered during FBJ. Since a large difference in martensite fraction between the HAZ and BM is hardly found, the lower hardness in the HAZ would be due to tempering of the martensite of the BM, which may be suggested by the carbide precipitation in the HAZ (Figure 5(f)). In the HAZ, the degree of tempering

should increase toward the TMAZ due to an increase in temperature. This would be a reason why the minimum hardness is found in the HAZ near the TMAZ.

IV. CONCLUSIONS

Friction bit joining successfully produced a defect-free spot weld in the DP980 steel using the bit made of the D2 tool steel. The joint had a heterogeneous hardness profile and microstructure distribution. The hardness profiles could be correlated with the microstructure distribution in the joint, and microstructural evolution of each region could be reasonably explained by both the stable phases at the maximum temperature and the solid-state phase transformation during the cooling cycle of FBJ.

ACKNOWLEDGMENTS

The authors are grateful to Messrs. M. Mosley and A. Honda for technical assistance. They also thank Mr. M. Matsunaga for helpful discussions. Financial support from the Japanese Ministry of Education, Science, Sports and Culture with a Grant-in-Aid from the Global COE program of the Materials Integration International Center for Education and Research at Tohoku University is gratefully acknowledged. Two of the authors (MPM and KK) acknowledge support from NSF Grant No. CMMI-0834729.

REFERENCES

1. N.T. Williams and J.D. Parker: *Int. Mater. Rev.*, 2004, vol. 49, pp. 45–75.
2. W.L. Chuko and J.E. Gould: *Weld. J.*, 2002, vol. 81, pp. 1-s–7-s.

3. X. Sun, E.V. Stephens, and M.A. Khaleel: *Eng. Fail. Anal.*, 2008, vol. 15, pp. 356–67.
4. T.B. Hilditch, J.G. Speer, and D.K. Matlock: *Mater. Des.*, 2007, vol. 28, pp. 2566–76.
5. S. Ferrasse, P. Verrier, and F. Meesemaeker: *Weld. World*, 1998, vol. 41, pp. 177–95.
6. L. Cui, H. Fujii, K. Nakata, K. Nogi, R. Ikeda, and M. Matsushita: *ISIJ Int.*, 2007, vol. 47, pp. 299–306.
7. L. Cui, H. Fujii, N. Tsuji, and K. Nogi: *Scripta Mater.*, 2007, vol. 56, pp. 637–40.
8. H. Fujii, L. Cui, N. Tsuji, M. Maeda, K. Nakata, and K. Nogi: *Mater. Sci. Eng. A*, 2006, vol. 429, pp. 50–57.
9. S.H.C. Park, Y.S. Sato, H. Kokawa, K. Okamoto, S. Hirano, and M. Inagaki: *Sci. Technol. Weld. Join.*, 2005, vol. 10, pp. 550–56.
10. Y.S. Sato, T.W. Nelson, and C.J. Sterling: *Acta Mater.*, 2005, vol. 53, pp. 637–45.
11. Y.S. Sato, T.W. Nelson, C.J. Sterling, R.J. Steel, and C.O. Pettersson: *Mater. Sci. Eng. A*, 2005, vol. 397, pp. 376–84.
12. Y.S. Sato, H. Yamanoi, H. Kokawa, and T. Furuhashi: *Scripta Mater.*, 2007, vol. 57, pp. 557–60.
13. S.H.C. Park, Y.S. Sato, H. Kokawa, K. Okamoto, S. Hirano, and M. Inagaki: *Scripta Mater.*, 2003, vol. 49, pp. 1175–80.
14. S.H.C. Park, Y.S. Sato, H. Kokawa, K. Okamoto, S. Hirano, and M. Inagaki: *Scripta Mater.*, 2004, vol. 51, pp. 101–05.
15. Y.S. Sato, H. Yamanoi, H. Kokawa, and T. Furuhashi: *ISIJ Int.*, 2008, vol. 48, pp. 71–76.
16. M.P. Miles, J. Pew, T.W. Nelson, and M. Li: *Sci. Technol. Weld. Join.*, 2006, vol. 11, pp. 384–88.
17. D. Mitlin, V. Radmilovic, T. Pan, J. Chen, Z. Feng, and M.L. Santella: *Mater. Sci. Eng. A*, 2006, vol. 441, pp. 79–96.
18. S. Lathabai, M.J. Painter, G.M.D. Cantin, and V.K. Tyagi: *Scripta Mater.*, 2006, vol. 55, pp. 899–902.
19. M. Fujimoto, N. Abe, Y.S. Sato, and H. Kokawa: *Q. J. Jpn. Weld. Soc.*, 2007, vol. 25, pp. 553–59.
20. M. Fujimoto, N. Abe, Y.S. Sato, and H. Kokawa: *Q. J. Jpn. Weld. Soc.*, 2008, vol. 26, pp. 67–73.
21. Z. Feng, M.L. Santella, S.A. David, and T.Y. Pan: *SAE Trans.*, 2005, vol. 114, pp. 592–98.
22. Y. Hovanski, M.L. Santella, and G.J. Grant: *Scripta Mater.*, 2007, vol. 57, pp. 873–76.
23. M.P. Miles, K. Kohkonen, S. Packer, R. Steel, B. Siemssen, and Y.S. Sato: *Sci. Technol. Weld. Join.*, 2009, vol. 15, pp. 72–77.
24. L. Bourithis, G.D. Papadimitriou, and J. Sideris: *Tribol. Int.*, 2006, vol. 39, pp. 479–89.
25. T.J. Lienert, W.L. Stellwag, B.B. Grimmett, and R.W. Warke: *Weld. J.*, 2003, vol. 82, pp. 1s–9s.
26. W.M. Thomas, P.L. Threadgill, and E.D. Nicholas: *Sci. Technol. Weld. Join.*, 1999, vol. 4, pp. 365–72.
27. N. Ozdemir, F. Sarsilmaz, and A. Hascalik: *Mater. Des.*, 2007, vol. 28, pp. 301–07.
28. A.Z. Sahin, B.S. Yibas, M. Ahmed, and J. Nickel: *J. Mater. Process. Technol.*, 1998, vol. 82, pp. 127–36.
29. L.W. Zhang, J.B. Pei, Q.Z. Zhang, C.D. Liu, W.H. Zhu, S. Qu, and J.H. Wang: *Acta Metall. Sinica*, 2007, vol. 20, pp. 301–06.
30. R.W.K. Honeycombe: *Steels Microstructure and Properties*, Edward Arnold, London, 1981, pp. 121–39.